ISSN: 0976-3376

Available Online at http://www.journalajst.com

ASIAN JOURNAL OF SCIENCE AND TECHNOLOGY

Asian Journal of Science and Technology
Vol. 07, Issue, 09, pp.3529-3544, September, 2016

RESEARCH ARTICLE

METAL COMPLEXES OF COMPARTMENTAL LIGANDS, SYNTHESIS, SPECTROSCOPIC CHARACTERIZATION AND CHEMOTHERAPEUTIC STUDIES

[1]Abdou Saad El-Tabl, [2]Moshira Mohamed Abd El-wahed, [3]Samar Ebrahim Abd-El Razek, [1]Sabreen Mohamed El Gamasy and [1]Eman Ahmed Mohamed

[1]Chemistry Department, Faculty of Science, Menoufia University, Shebin El-Kom, Egypt
[2]Pathology Department, Faculty of Medicine, Menoufia University, Shebin El-Kom, Egypt
[3]Clinical Pathology Department, National Liver Institute, Menoufia University, Shebin El-Kom, Egypt

ARTICLE INFO

Article History:
Received 29th June, 2016
Received in revised form
22nd July, 2016
Accepted 09th August, 2016
Published online 30th September, 2016

Key words:

Metal complexes,
Preparation, Spectroscopic
Characterization antitumor and
antimicrobial studies.

ABSTRACT

New series of symmetric and asymmetric binuclear Cu(II), Ni(II), Co(II), Mn(II), Zn(II), Fe(III), Cd(II) and Cr(III) complexes with newly synthesized ligand 4, 6-bis-[1-(2-hydroxy-ethylimino)-ethyl]-benzene-1, 3-diol have been synthesed. The ligand and its metal complexes have been characterized using IR, Mass, ^{1}H NMR, UV–Vis., elemental analysis, conductance, magnetic moments, ESR and Thermal gravimetric analyses (DTA – TGA). Elemental and spectral data indicate octahedral structures for the prepared complexes. Molar conductances in DMF commensurate non- electrolyte. The ligand and its metal complexes show antitumor inhibitory activity against hepatocellular carcinoma (HepG-2 cell line). Also, the ligand and its complexes were screened for antibacterial activity against two Gram-negative bacteria including *Escherichia coli* and gram-positive bacteria such as *Bacillis subtilis* and *Streptococcus pneumonia* using the disc diffusion and micro Broth dilution assays. Also, the same complexes were tested against fungi including *Aspergillus fumigatus* and *Candida albicans.*

Copyright©2016, Abdou Saad El-Tabl et al. *This is an open access article distributed under the Creative Commons Attribution License, which permits unrestricted use, distribution, and reproduction in any medium, provided the original work is properly cited.*

INTRODUCTION

Schiff base complexes are considered as their ability to reversibly binding oxygen in epoxidation reactions, biological activity, complexing ability towards some toxic metals and catalytic activity in hydrogenation of olefins and photochromic properties (Chang *et al.,* 2006; Nagesh *et al.,* 2015; Naiya *et al.,* 2011 Zayed *et al.,* 2015; Rahaman and Mruthyunjayaswamy, 2014). The N and O donor atoms present in the Schiff base biological systems represent an important role in metalloproetins and metallo-enzymes. Indole derivatives have been widely used in making perfumes, dyes, herbicides, agrochemicals and medicines (Sakamoto *et al.,* 1990; Raman and Sobha, 2012; Zafar *et al.,* 2015; Kumar *et al.,* 2015). The metal binding ability allows for Schiff base compounds to be used as ligands in coordination chemistry. Schiff base complexes are considered as their ability to reversibly binding oxygen in epoxidation reactions, biological activity, complexing ability towards some toxic metals and catalytic activity in hydrogenation of olefins and photochromic properties (Chang *et al.,* 2006; Nagesh *et al.,* 2015; Naiya *et al.,* 2011 Zayed *et al.,* 2015; Rahaman and Mruthyunjayaswamy, 2014). Schiff base complexes have been extensively studied because of its important significance in biochemical, analytical and antimicrobial reagents (Klement *et al.,* 1999). Schiff bases complexes hold potential in the design of new anticancer agents (Omar, 2009). In this present investigation, we studied a simple synthetic method to synthesize a Schiff base ligand and its metal complexes. The structure of these compounds was elucidated by analytical and spectroscopic methods. Also, the antimicrobial and anticancer activities were studied successfully.

****Corresponding author: Abdou Saad El-Tabl,***
Chemistry Department, Faculty of Science, Menoufia University, Shebin El-Kom, Egypt

Experimental

MATERIALS AND METHODS

All the reagents were of the best grade available and used without further purification.

Physical measurements

C, H, N and Cl analyses were determined at the Analytical Unit of Cairo University, Egypt. A standard method

[gravimetric] was used to determine metal (II)/(III) ions (Vogel, 1961). All complexes were dried under vacuum over P_4O_{10}. The IR spectra were measured as KBr and CeBr pellets using a Perkin-Elmer 683 spectrophotometer (4000-200 cm^{-1}). Electronic spectra were recorded on a Perkin-Elmer 550 spectrophotometer. The conductance of (10^{-3} M DMF) of the complexes were measured at 25°C with a Bibby conductimeter type MCl. ^{1}H-NMR spectra were obtained with Perkin-Elmer R32-90-MHz spectrophotometer using TMS as internal standard. Mass spectra were recorded using JEULJMS-AX-500 mass spectrometer provided with data system. The thermal analyses (DTA and TGA) were carried out in air on a Shimadzu DT-30 thermal analyzer from 27 to 800°C at a heating rate of 10°C per minute. Magnetic susceptibilities were measured at 25°C by the Gouy method using mercuric tetrathiocyanato cobalt(II) as the magnetic susceptibility standard. Diamagnetic corrections were estimated from Pascal's constant [13]. The magnetic moments were calculated from the equation:

$$\mu_{eff} = 2.84\sqrt{\chi_M^{corr}.T}$$

The ESR spectra of solid complexes at room temperature were recorded using a varian E-109 spectrophotometer, DPPH was used as a standard material. The T.L.C of the ligand and its complexes confirmed their purity.

Preparation of the ligand and its metal complexes
Preparation of the ligand, [H_2L] (1)

Ligand (1) was prepared by refluxing with stirring equimolar amounts of 4,6_Diacetyl resorcinol (10 g, 0.051 mol) and ethanol amine (6.29 g, 1029 mol) [1:2] in ethanol (100 cm^3) for 2 hrs. The deep brown product obtained was filtered off, then washed several times with ethanol and dried in vacuum over P_4O_{10}. Analytical data are given in Table (1).

Preparation of metal complexes (2)-(24)

A filtered ethanolic (100 cm^3) (7.13 g, 0.035 mol) of $Cu(OAc)_2.H_2O$, was added to an ethanolic (100 cm^3) of the ligand, (1) (5.0 g, 0.017 mol) [1L:2M], complex (2), (5.7 g, 0.035 mol) of $CuSO_4$, [1L:2M], complex (3), (4.8 g, 0.035 mol) of $CuCl_2$, [1L:2M], complex (4), (8.89 g, 0.035 mol) of $Ni(OAc)_2.4H_2O$, [1L:2M], complex (5), (9.39 g, 0.035 mol) of $NiSO_4.6H_2O$ [1L:2M] complex (6), (4.54 g, 0.035 mol) of $Ni(Co_3)_2.2H_2O$,[1L: 2M], complex (7), (8.89 g, 0.035 mol) of $Co(OAc)_2.4H_2O$, [1L:2M], complex (8), (0.035 mol) of $CoSO_4$, [1L:2M], complex (9), (4.64, 0.035 mol) of $CoCl_2.4H_2O$, [1L:2M], complex (10), (8.75, 0.035 mol) of $Mn(OAc)_2.4H_2O$, [1L:2M], complex (11), (6.04, 0,035 mol) of $MnSO_4.H_2O$, [1L:2M], complex (12), (0.035 mol) of $MnCO_3.2H_2O$, [1L:2M], complex (13), (7.84, 0.035 mol) of $Zn(OAc)_2.2H_2O$, [1L:2M], complex (14), (0.035 mol) of $ZnSO_4.H_2O$, [1L:2M], complex (15), (0.035 mol) of $FeSO_4$, [1L:2M], complex (16), (, 0.035 mol) of $Cr_2(SO_4)_3$, [1L:2M], complex (17), (9.52, 0.035 mol) of $Cd(OAc)_2.H_2O$, [1L:2M], complex (18), (9.16, 0.035 mol) of $CdSO_4$, [1L:2M], complex (19), (0.035 mol) of $CdCl_2.H_2O$, [1L:2M], complex (20), (3.57, 3.12 , 0.017 mol) of Cu-Zn, [1L:1M:1M], complex (21), (3.92, 4.43, 0.017 mol) of $Ni(OAc)_2.4H_2O$ / $Zn(OAc)_2.2H_2O$, [1L:1M:1M], complex (22), (3.92, 4.38, 0.017 mol) of $Mn(OAc)_2.4H_2O$/ $Zn(OAc)_2.2H_2O$, [1L:1M:1M], complex (23), (3.92, 4.45, 0.017 mol) of $CoCl_2.4H_2O$ / $Zn(OAc)_2.2H_2O$ [1L:1M:1M], complex (24). The mixture was refluxed with stirring for 1-3hrs, depending on the nature of metal salts, the coloured complex was filtered off, washed with ethanol and dried under vacuo over P_4O_{10}.

Biological activities

Antitumor activity

The antitumor action was measured in vitro for the synthesized metal complexes according to Sulfo-Rhodamine-B-stain (SRB) assay using the published methods (Skehan *et al.,* 1990). Cells were plated in 96-multiwell plate (10^4 cells/well) for 24 hrs before treatment with the metal complexes to allow attachment of cell to the wall of the plate. Different concentrations of the metal complexes in DMSO (1.56, 3.125, 6.25, 12.5, 25 and 50 µg /ml) were added to the cell monolayer triplicate. Monolayer cells were incubated with the metal complexes for 48 hrs at 37°C using of 5% CO_2. After 48 hrs, cells were fixed, washed and stained with Sulfo-Rhodamine-B-stain. Excess stain was wash with acetic acid and attached stain was recovered with tris EDTA buffer (10 m M tris HCl + 1 m M disodium EDTA, PH 7.5-8). Color intensity was measured by ELISA reader. The relation between surviving fraction and drug concentration is plotted to get the survival curve of each tumor cell line after the specified metal complex. Sorafenib is used as a standard drug.

Antibacterial action (In Vitro)

The ligand and its metal complexes have been studied against one Gram-negative bacteria including *Escherichia coli* (RCMB 010052) and two Gram-positive bacteria such as *Bacillis subtilis* (RCMB 010067) and *Streptococcus pneumoniae* (RCMB 010010) using disc diffusion based on Muller-Hinton agar medium (Merck, Germany) (El-Tabl *et al.,* 2013). The sterile petri plates containing Muller Hinton agar medium are fertilized with 0.1 ml of the specific bacterium, which included nearly 0.5 x 10^6 (CFU/ml) (equal to 0.5 McFarland standards) (Chohan *et al.,* 2010). On the other hand, sterile disks (6 mm in diameter) have been soaked at samples with different concentrations (5, 2.5, 1.25 mg/disk in DMSO) and located on the agar plates. Entire plates were incubated at 37^0 C for 24 hrs. After the suffient time, inhibitory zone diameter (mm) of each chelate was appeared measured and reported as the antibacterial activity. In accordance with some other reports in literature, DMSO exhibited no effect at the same biological environment (Chohan *et al.,* 2010; Durai Anad *et al.,* 2008). Some commercial antibiotics such as *Gentamicin* and *Ampicillin* used as positive controls references.

Minimum inhibitory concentration

Beside the disk diffusion method, MIC has used as the next method to apprising antibacterial activites of our synthetic metal complexes. For this test, various concentrations of the complexes through serial dilution (1000 to 31.25 µg/ml) were prepared in sterile test tube and then 650 µl of sterile Muller-Hinton broth medium (Scharlab) and 100µl of the specific bacterium were added to them and finally entire ones

incubated at 37^0 C for 24 hrs. According to the observation of test tubes, the lowest concentration of each complex, which inhibited visible growth of bacteria, is reported as MIC of it (Sedighinia *et al.,* 2012).

Antifungal activity

Fungicidal activity of tested complexes was assessed against Aspergillus fumigatus and Candida albicans by disc diffusion method. Base layer was obtained by pouring about 10-15 ml of base layer medium into each sterilized petri dishes and were allowed to attain at room temperature. Overnight grown subcultures of fungi were mixed with layer medium and immediately poured into petri dishes containing the base layer and then allowed to attain at room temperature. Antifungal discs having diameter of 6mm, soaked in test solution, were dispensed on to the surface of inoculated agar plate. Each disc must be pressed down to ensure its complete contact with the agar surface. These plates were subsequently incubated at 37 ^{0}C for 36 hrs. The zone of inhibition, if any, was measured in mm for the particular complex. Clotrinazole was used as positive control and solvent control (12mm) was also used to know the activity of the solvent.

RESULTS AND DISCUSSION

All the complexes are stable at room temperature, non hydroscopic, insoluble in water and partially soluble in common organic solvents such as $CHCl_3$, but soluble in DMF and DMSO. The analytical and physical data of the ligand and its complexes are given in Table (1), spectral data Tables (2-6) are compatible with the proposed structures, Figure (1). The molar conductances are in the 6.2 - 16.3 $ohm^{-1}cm^2mol^{-1}$ range, Table (1), indicating a non-electrolytic nature (Geary, 1971). The high value for some complexes suggests partial dissociation in DMF. Reaction of (1) with metal salts using (1L: 2M) and (1L:1M:1M) molar ratios in ethanol gives complexes (2)-(24). The composition of the complexes formed depends on metal salts and the molar ratios.

^{1}H-NMR spectra

The ^{1}H-NMR spectra of the ligand and its Zn(II) complex (14) and Cd(II) complex (18) in deuterated DMSO show signals consistent with the proposed structure. The spectrum of the ligand shows protons of chemical shift observed as a singlet at 9.85 and 9.78 ppm, is assigned to proton of phenolic and hydroxyl groups (El-Tabl *et al.,* 2007; Kantekin *et al.,* 2004; Plass *et al.,* 2009). Resonances appeared in the 4.05-4.26 ppm range are due to methyl attach to imino group (El-Tabl *et al.,* 2007; Plass *et al.,* 2009; Gudasi *et al.,* 2006). Also, the spectrum showed a set of peaks as multiples at 6.68-7.35 ppm range which are assigned to the protons of aromatic ring (El-Tabl *et al.,* 2010). Methylene protons of CH_2 group appeared at 2.35-3.64 ppm range which observed as multiple ones (Gudasi *et al.,* 2006). However, for Zn(II) complex (14) and Cd(II) complex (18). signals appeared at nearly the same positions of the hydroxyl groups indicate non participating in coordination to the metal ions. Also, set of peaks appeared as multiples at 6.28-7.48 and 6.03-7.33 ppm ranges are corresponding to protons of aromatic ring, respectively (El-Tabl *et al.,* 2010). The signals appeared at 3.47-4.27 and 3.36-4.35 ppm ranges are due to methyl attach to imino group, respectively (El-Tabl *et al.,* 2010). The appearance of new signals at 1.89 and 1.79 ppm is due to protons of coordinated acetate groups, respectively (Baligar *et al.,* 2006).

Mass spectra

The mass spectra of the ligand and its Co(II) complex (10), Fe(III) complex (16) and Cu(II)-Zn(II) complex (21) confirmed their proposed formulations. The spectrum of ligand reveals the molecular ion peaks (m/z) at 280 amu consistent with the molecular weight of the ligand (280). Furthermore, the fragments observed at m/z = 45, 86, 177, 194, 235 and 280 correspond to C_2H_5O, C_4H_8NO, $C_{10}H_{11}O_2N$, $C_{10}H_{12}NO_3$, $C_{12}H_{15}N_2O_3$ and $C_{14}H_{20}N_2O_4$ moieties, respectively. However, the Co(II) complex (10) shows peak (m/z) at 610.7 amu. Additionally, the peaks observed at 45, 86, 250.35, 340.35, 488.7, 574.7 and 610.7 are due to C_2H_5O, C_4H_8ON, $C_4H_{14}NO_5ClCo$, $C_{10}H_{16}NO_6ClCo$, $C_{10}H_{22}NO_9Co_2Cl_2$, $C_{14}H_{30}N_2O_{10}Co_2Cl_2$ and $C_{14}H_{34}N_2O_{12}Co_2Cl_2$ moieties, respectively. Also, the Fe(III) complex (16) shows peak (m/z) at 725.68 amu. Additionally, the peaks observed at 45, 86, 307.84, 381.84, 603.68, 689.68 and 725.68 are due to C_2H_5O, C_4H_8ON, $C_4H_{14}NO_9Fe$, $C_{10}H_{16}NO_9Fe$, $C_{10}H_{22}NO_{17}Fe_2$, $C_{14}H_{30}N_2O_{18}Fe_2$ and $C_{14}H_{34}N_2O_{20}Fe_2$, moieties, respectively. However, the Cu(II)-Zn(II) complex (21) shows peak (m/z) at 669.44 amu. Additionally, the peaks observed at 45, 86, 278.54, 352.54, 547.44, 633.44 and 669.44 are due to C_2H_5O, C_4H_8ON, $C_6H_{17}NO_7Cu$, $C_{12}H_{19}NO_7Cu$, $C_{14}H_{28}NO_{13}ZnCu$, $C_{18}H_{36}N_2O_{14}ZnCu$ and $C_{18}H_{40}N_2O_{16}ZnCu$ moieties, respectively as shown in Table (2).

IR spectra

The IR spectra of the ligand and its complexes (2) - (24) are given in Table (3). The spectrum of (1) showed ν(OH) bands at 3420 and 3331 cm^{-1}, the appearance of two broad bands at 3640-3220 and 3130-2708 cm^{-1} ranges, commensurate the presence of two types of intra-and intermolecular hydrogen-bonding (El-Tabl, 1997; Dongli *et al.,* 1994). Thus, the higher frequency band is associated with a weaker hydrogen bond and the lower frequency band with a strong hydrogen bond. Also, the spectrum shows bands at 1652 cm^{-1} assigned to $\nu(C=N)_{imine}$ group (Tas *et al.,* 2005, 1999; El-Behry, 2007). P-substitued aromatic ring appears at 1580 and 870 cm^{-1} (Nakatamato, 1967). The IR spectra of the complexes show, the $\nu(C=N)_{imine}$ stretching frequency undergoes a shift to lower frequency by (17 - 44) cm^{-1}. This is indicative of nitrogen coordination of the azomethine to the metal ion [33, 34]. The bands observed in the 1505-1590 and 730-870 cm^{-1} ranges are due to aromatic group (El-Tabl, 1997; Nakatamato, 1967; El-Tabl, 2002). However, complexes (2)-(24) show medium band in the 3306-3488 cm^{-1} range is due to ν(OH) group ((El-Tabl, 1997; Nakatamato, 1967). Complexes show broad bands in the 3694-3108 and 3368-2380 cm^{-1}, ranges, corresponding to intra-and intermolecular hydrogen bondings (El-Tabl, 1997; Dongli *et al.,* 1994). However, the hydrated and coordinated water molecules appear in the 3670-3205 and 3385-2770 cm^{-1} ranges (El-Tabl *et al.,* 2003, 2007; Hegazy, 2001). Extensive IR spectral studies reported on metal acetate complexes (Nakatamato, 1967; El-Tabl, 2002) indicate that, the acetate ligand coordinates in either a monodentate or bidentate manner, the $\nu_a(COO)$ and $\nu_s(COO)$ of the free acetate are observed at 1560 and 1416 cm^{-1} respectively.

In complexes (2), (5), (8), (11), (14), (18), (21), (22), (23) and (24), the band is due to ν_{as}(COO) appears in the 1487-1427 cm^{-1} and the ν_s(COO) observed in the 1370-1320 cm^{-1} ranges. The difference between these two bands is in the 117-107 cm^{-1} range, suggesting that, the acetate group coordinates in unidentate manner with the metal ion (Nakatamato, 1967; El-Tabl, 2002; Fouda *et al.,* 2008). Complexes (3), (6), (9), (12), (15), (16), (17) and (19) show bands at 1289-1246, 1190-1150 and 789-658cm^{-1} ranges, respectively are corresponding to monodentate coordinate sulphate group (Kuska and Rogers, 1971). Complexes (4), (10) and (20) show bands at 470-450 cm^{-1}, assigened to ν(M-Cl) (El-Bahnasawy *et al.,* 1995). Complexes (7) and (13) show bands at 1535, 1370, 760 and 1588, 1340, 789 cm^{-1}, assigned to coordinated carbonate group respectively (Nakatamato, 1967).

Magnetic moments

The magnetic moments of the complexes (2)-(24) are shown in Table (4). Cu(II) complexes (2)-(4) show values 1.60-1.76 B.M range, corresponding to one unpaired electron in an octahedral structure, complexes (3) shows values which are well below the spin only value (1.73 B.M), indicating that, spin-exchange interactions take place between the Cu(II) ion through intermolecular hydrogen bondings in an octahedral geometry (Gudasi, 2006). Ni(II) complexes (5)-(7) show values 3.39, 3.29 and 3.26 B.M., respectively, indicating an octahedral geometry around Ni(II) ion (Motaleb *et al.,* 1997). Co(II) complexes (8)-(10) show values 4.72, 4.71 and 4.83 B.M., respectively, indicating high spin octahedral Co(II) complexes (Al-Hakimi *et al.,* 2011). Mn(II) complexes (11-13) show values 5.11, 5.08 and 5.23 B.M., respectively, suggesting high spin octahedral geometry around the Mn(II) ion (Al-Hakimi *et al.,* 2011). Fe(III) complex (16) and Cr(III) complex (17) show values 5.18 and 2.32 B.M., respectively, indicating high spin octahedral structure (Al-Hakimi *et al.,* 2011). Zn(II), complexes (14) and (15) and Cd(II) complexes (18)-(20), show diamagnetic property (El-Tabl, 1997). Complexes (21)-(24) show values 1.72, 2.86, 5.16 and 4.22 B.M, respectively, indicating octahedral structure around the metal ion.

Electronic spectra

The electronic spectral data for the ligand and its complexes in DMF solution are summarized in Table (4). Ligand in DMF solution shows bands at 400 nm and 295 nm which may be assigned to the n→π* and π→π* transitions respectively (Gudasi *et al.,* 2006). Cu(II) complexes (2)-(4) show bands in the 295– 270, 318–302 and 390–350 nm ranges, these bands are due to intraligand transitions, however, the bands appear in the 456–430, 560–510 and 650 –600 nm ranges are assigned to O→Cu charge transfer, $^2B_1 \rightarrow {}^2E$ and $^2B_1 \rightarrow {}^2B_2$ transitions, indicating a distorted tetragonal octahedral structure (El-Tabl *et al.,* 2004). Ni(II) complexes (5)-(7) show bands 270, 313, 390, 505, 630 and 725 and 275, 320, 380, 525, 635, 730 and 280, 310, 370, 515, 605 and 720 nm, respectively, the first three bands are within the ligand and the other three bands are attributable to $^3A_{2g}(F) \rightarrow {}^3T_{1g}(P)(\nu_3)$, $^3A_{2g}(F) \rightarrow {}^3T_{1g}(F)(\nu_2)$ and $^3A_{2g}(F) \rightarrow {}^3T_{2g}(F)(\nu_1)$ transitions respectively, indicating an octahedral Ni(II) complex [47, 50]. The ν_2/ν_1 ratio for the complexes is 1.25, 1.19 and 1.17, which are less than the usual range of 1.5–1.75, indicating distorted octahedral Ni(II) complexes (El-Tabl *et al.,* 2004; Chinvmia *et al.,* 1995). Co(II) complexes (8)-(10) show bands at 270, 320, 375, 553, 628 and 278, 310, 376, 580, 620 and 275, 310, 360, 580, 650 nm, the first three bands are within the ligand and the other bands are assigned to $^4T_{1g}(F) \rightarrow {}^4A_{2g}$ and $^4T_{1g}(F) \rightarrow {}^4T_{2g}(F)$ transitions, respectively, corresponding to high spin Co(II) octahedral complexes (Krishna *et al.,* 1997). Mn(II) complexes (11)-(13) show bands at 270, 325, 370, 445, 565 and 270, 320, 378, 490, 558 and 277, 315, 410, 560 nm, respectively, the first three bands are within the ligand, however, the other bands are corresponding to $^6A_{1g} \rightarrow {}^4E_g$, $^6A_{1g} \rightarrow {}^4T_{2g}$ and $^6A_{1g} \rightarrow {}^4T_{1g}$ transitions which are compatible to an octahedral geometry around the Mn(II) ion (Parihari *et al.,* 2000). Zn(II) complexes (14) and (15) show bands at 270, 280, 320, 395 and 260, 290, 320, 380 which are assigned to intraligand transitions. Fe(III) complex (16) shows bands at 260, 335, 394, 465, 580 and 660 nm, respectively, the first three bands are within the ligand while the other bands are due to charge transfer and $^6A_1 \rightarrow {}^4T_1$ transitions, suggesting distorted octahedral geometry around the Fe(III) ion (El-Tabl *et al.,* 2008; Sing, 2001). While Cr(III) complex (17) shows bands at 285, 318, 389, 470, 560 and 630 nm, respectively. The first three bands are within the ligand and the other bands are assigned to $^4A_{2g} \rightarrow {}^4T_{1g}(F)$, $^4A_{2g} \rightarrow {}^4T_{2g}$ and $^4A_{2g} \rightarrow {}^2T_{2g}$ transitions respectively, indicating octahedral structure around the Cr(III) ion (Abu *et al.,* 1990; Lever, 1968). Cd(II) complexes (18)- (20) show three bands in the 290–260, 315–330 and 370–410 nm ranges, which are assigned to intraligand transitions. However, complexes (21)-(24) show bands at 260-285, 315-360 and 385-395 nm, respectively, indicating interligand transitions. The other bands confirmed octahedral structure for Cu(II), Ni(II), Co(II) and Mn(II) complexes.

Electron spin resonance (ESR)

The ESR spectral data for complexes (2), (3), (4), (8), (9), (11) and (12) are presented in Table (5). The spectra of Cu(II) complexes (2), (3) and (4) are characteristic of species, d^9 configuration and having axial type of a $d_{(x2-y2)}$ ground state which is the most common for Cu(II) complexes (El-Tabl, 2004, 2011). The complexes show $g_{\|} > g_{\perp} > 2.0023$, indicating octahedral geometry around Cu(II) ion [60, 61]. The g-values are related by the expression (El-Boraey, 2003; Procter *et al.,* 1969). $G=(g_{\|}-2)/(g_{\perp}-2)$, if G > 4.0, then, local tetragonal axes are aligned parallel or only slightly misaligned, if G < 4.0, the significant exchange coupling is present. Also, the $g_{\|}/A_{\|}$ values are considered as a diagnostic of stereochemistry (Nickless, 1983). The $g_{\|}/A_{\|}$ values lie just within the $\perp$ range expected for the complexes Table (5). The orbital reduction factors ($K_{\|}$, K, K), which are a measure of covalency can be calculated (Ray, 1990). K Table (5), for the Cu(II) complexes (2), (3) and (4), indicating covalent bond character (El-Tabl, 2004). The g-values reported here Table (5) show considerable covalent bond character [66, 67]. Also, the in-p lane σ- covalency parameter, α^2(Cu) Table (5) suggests a covalent bonding [65]. The complexes show show $ß_1^2$ values and indicating a covalency in the in-plane π-bonding [60, 65, 68]. While $ß^2$ for complexes (2) and (3) are 0.67 and 0.76 respectively, indicating covalent bonding character out of- plane π- bonding, however, complex (4) shows 0.89 indicating ionic character of the out of- plane (El-Tabl, 2000; Bhadbhade, 1993). The calculated orbital populations (a^2_d) for the Cu(II) complexes (2), (3) and (4),

Table (5), indicate a $d_{(x2-y2)}$ ground state (Symons, 1979; El-Tabl, 2002). Co(II) complexes (8) and (9) and Mn(II) complexes (11) and (12) show isotropic spectra with values 2.09, 2.1, 2.007 and 2.009 respectively indicating octahedral structures.

Thermal analyses (DTA and TGA)

The thermal curves in the temperature 27-800°C range for complexes (2), (3), (10), (14) and (20) are thermally stable up to 40°C. Endothermic peak appeared around 50°C with no weight loss may be due to broken of H- bondings. Complexes show endothermic peaks within temperature 50-60°C range, is due to elimination of hydrated water (El-Tabl, 1997; Gaber and Ayad, 1991) ($2H_2O$, (2), (3), (10), (14) and (20)). Another endothermic peaks within 108-174°C range, is due to loss of coordinated water ($6H_2O$, (2), (3), (10), (14) and (20)) in (table 6). Complex (2) shows one endothermic peak at 230°C with 22.46% weight loss (Calc. 22.56%), corresponding to the loss of two coordinated acetate group. Endothermic peak observed at 379^oC may be due to melting point. Finally, the complex shows exothermic peaks at 390, 424, 490, 617 and 799°C, with 39.02% weight loss (Calc. 39.27%) corresponding to oxidative thermal decomposition which proceeds slowly with final residue assigned to 2CuO. Complex (3) shows endothermic peaks at 250, 165°C, with 31.83% weight loss (Calc. 32.04%) are due to loss of two coordinated sulphate groups. The endothermic peak observed at 373°C may be assigned to the melting point. Oxidative thermal decomposition occurs at 480, 568 and 619°C, with 38.81% weight loss (Calc. 39.07%) with exothermic peaks, leaving 2CuO (El-Tabl, 1999). Complex (10) shows endothermic peak at 245°C, with 15.05% weight loss (Calc. 15.19%) is due to loss of two chloride anions. The endothermic peak observed at 320°C may be due to melting point. Oxidative thermal decomposition occurs at 385, 444, 537 and 635°C, with 37.56% weight loss (Calc. 37.85%) with exothermic peaks, leaving 2CoO. Complex (14) shows endothermic peak at 233°C, with 22.2% weight loss (Calc. 22.36%) is due to loss of two coordinated acetate groups. Also another endothermic peak observed at 370^oC is due to melting point. Oxidative thermal decomposition occurs at 390, 407, 557 and 684°C, with 39.78% weight loss (Calc. 39.97%) with exothermic peaks, leaving 2ZnO. Finally, complex (20) shows endothermic peak at 237^0C with 12.03% weight loss (Calc. 12.36%) is due to loss of two chloride anions. At 356^0C, endothermic peak appears which is due to melting point. Oxidative thermal decomposition occurs at 394, 465, 523 and 744^0C, with 50.78% weight loss (Calc. 51.07%) with exothermic peaks, leaving 2CdO. The thermal data are present in Tabe (6).

Biological studies

Antitumor activity

The antitumor activity of the ligand, (1) and its metal complexes (3), (4), (10), (11), (12), (16) and (17) in DMSO were evaluated against HepG-2 cell line. These were tested by comparing them with the standard drug (Sorafenib). The solvent DMSO showed no effect on cell growth as it reported previously (Illan *et al.,* 2005). The ligand (1), showed a strong inhibition effect at 50 µg /ml of concentration used, also, the metal complexes (3), (12) and (16) showed strong effect against HepG-2 cell line at 50 µg /ml, but complex (12) has more effective than standard at 3.125 and 1.56 µg /ml compared with standard, as shown in Figure (2). There was a positive correlation between the surviving fraction ratio of HepG-2 tumor cell line and the concentration. This could be explained as follow metal ion could binds to DNA where it seemed that, change the anion and the nature of the metal ion in complexes may have effect on the biological behavior, by altering the binding ability of DNA (Illan *et al.,* 2005; Hall *et al.,* 1997). Moreover, Gaetke and Chow had reported that, metal has been suggested to facilitate oxidated tissue injury through a free-radical mediated pathway analogous to the Fenton reaction. By applying the ESR-trapping technique, evidence for metal-mediated hydroxyl radical formation invivo has been obtained (El-Tabl, 2004). Radicals are produced through a Fenton-type reaction as follows (Gaetke, 2003)

$$LM(II) + H_2O_2 \rightarrow LM(I) + {}^{\cdot}OOH + H^+$$
$$LM(I) + H_2O_2 \rightarrow LM(II) + {}^{\cdot}OH + OH^-$$

Where L is the ligand

Also, metal could act as a double-edged, sword by inducing DNA damage and also by inhibiting their repair [80]. The OH radicals react with DNA sugars and bases and the most significant and well-characterized of the OH reactions is hydrogen atom abstraction from the C_4 atom to yield sugar radicals with subsequent β-elimination. Scheme (1), by this mechanism strand breakage occurs as well as the release of the free bases. Another form of attack on the DNA bases is by solvated electrons, probably via a similar reaction to those discussed below for the direct effects of radiation on DNA (Smith, 1971).

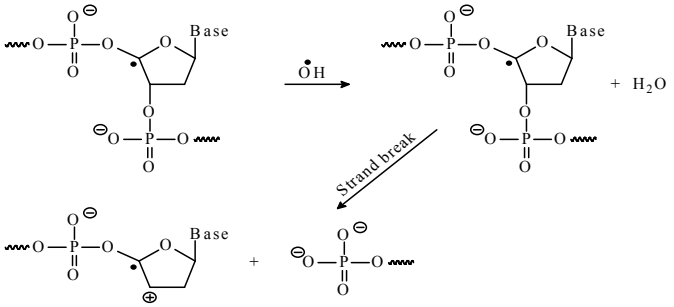

Scheme (1)

Intercalative binding of metal complex to DNA resulting from the insertion of metal complex between the base pairs of the DNA double helix. The binding mode depends on agreat extent not only on the nature of the metal ion but on the presence of the neighboring donor group in the same complex rings upon coordination to metal ion (Duda *et al.,* 1997; Custot *et al.,* 1995). The IC_{50} values were in the 3.79 - 30 µg range against human hepatocellular carcinoma cells (HepG-2) as shown in Figure (9). The relation between the concentration of the complexes in DMSO and their antitumor activities are shown in Table (7) and Figures (3-8).

Antibacterial activity

In vitro biological screening tests of the ligand (1) and its metal complexes were carried out as antibacterial activity.

Table 1. Analytical and physical data of the ligand [H_2L] (1) and its metal complexes

No.	Ligands/ Complexes	Color	FW	M.P (^{0}C)	Yield (%)	Anal. /Found (Calc.) (%)				Molar conductance
						C	H	N	M	
(1)	[H_2L]	Deep	280	>300	79	60.00	7.41	10	-	_
	$C_{14}H_{20}N_2O_4$	Brown				(59.81)	(6.94)	(9.84)		
(2)	[(L)$(Cu)_2(OAc)_2(H_2O)_6$].2H_2O	Brown	667.08	>300	72	32.38	5.99	4.19	19.05	6.5
	$C_{18}H_{40}Cu_2N_2O_{16}$					(32.05)	(5.64)	(4.05)	(18.84)	
(3)	[(H_2L)$(Cu)_2(SO_4)_2(H_2O)_6$].2H_2O	Brown	743.08	>300	70	22.61	4.84	3.77	17.1	6.3
	$C_{14}H_{36}Cu_2N_2O_{20}S_2$					(22.52)	(4.46)	(3.51)	(16.86)	
(4)	[(L)$(Cu)_2(Cl)_2(H_2O)_6$].2H_2O	Brown	619.98	>300	77	27.09	5.48	4.52	20.49	6.2
	$C_{14}H_{34}Cu_2N_2O_{12}Cl_2S_2$					(26.59)	(5.34)	(4.4)	(20.39)	
(5)	[(L)$(Ni)_2(OAc)_2(H_2O)_6$].2H_2O	Brown	657.38	>300	68	32.86	6.08	4.26	17.86	11.2
	$C_{18}H_{40}Ni_2N_2O_{16}$					(32.51)	(5.84)	(4.05)	(17.56)	
(6)	[(H_2L)$(Ni)_2(SO_4)_2(H_2O)_6$].2H_2O	Brown	733.38	>300	74	22.91	4.91	3.82	16.01	12.1
	$C_{14}H_{36}Ni_2N_2O_{20}S_2$					(22.59)	(4.55)	(3.64)	(15.84)	
(7)	[(H_2L)$(Ni)_2(CO_3)_2(H_2O)_6$].2H_2O	Brown	661.38	>300	70	29.03	5.44	4.23	17.75	10.8
	$C_{16}H_{36}Ni_2N_2O_{18}$					(28.85)	(5.3)	(4.02)	(17.64)	
(8)	[(L)$(Co)_2(OAc)_2(H_2O)_6$].2H_2O	Brown	657.8	>300	68	32.84	6.08	4.26	17.91	12.9
	$C_{18}H_{40}Co_2N_2O_{12}$					(32.54)	(5.86)	(4.05)	(17.63)	
(9)	[(H_2L)$(Co)_2(SO_4)_2(H_2O)_6$].2H_2O	Brown	733.8	>300	67	22.89	4.91	3.82	16.05	11.1
	$C_{14}H_{36}Co_2N_2O_{20}S_2$					(22.63)	(4.52)	(3.72)	(15.84)	
(10)	[(L)$(Co)_2(Cl)_2(H_2O)_6$].2H_2O	Brown	610.7	>300	55	27.51	5.57	4.58	19.29	12.8
	$C_{14}H_{34}Co_2N_2Cl_2O_{12}$					(27.5)	(5.46)	(4.46)	(19.05)	
(11)	[(L)$(Mn)_2(OAc)_2(H_2O)_6$].2H_2O	Brown	649.86	>300	77	33.24	6.16	4.31	16.91	12.9
	$C_{18}H_{40}Mn_2N_2O_{16}$					(33.02)	(6.05)	(4.22)	(16.56)	
(12)	[(H_2L)$(Mn)_2(SO_4)_2(H_2O)_6$].2H_2O	Brown	725.86	>300	68	23.14	4.96	3.86	15.14	11.9
	$C_{14}H_{36}Mn_2N_2O_{20}S_2$					(23.05)	(4.63)	(3.65)	(14.84)	
(13)	[(H_2L)$(Mn)_2(Co_3)_2(H_2O)_6$].2H_2O	Brown	653.86	>300	65	29.36	5.51	4.28	16.8	10.7
	$C_{16}H_{36}Mn_2N_2O_{18}$					(29.05)	(5.19)	(4.1)	(16.65)	
(14)	[(L)$(Zn)_2(OAc)_2(H_2O)_6$].2H_2O	Brown	671.8	>300	70	32.15	5.95	4.17	19.62	8.89
	$C_{18}H_{40}Zn_2N_2O_{16}$					(31.85)	(5.45)	(3.98)	(19.46)	
(15)	[(H_2L)$(Zn)_2(SO_4)_2H_2O)_6$].2H_2O	Brown	747.8	>300	80	22.47	4.81	3.74	17.63	13.85
	$C_{14}H_{36}Zn_2N_2O_{20}S_2$					(22.35)	(4.63)	(3.43)	(17.45)	
(16)	[(L)$Fe_2(SO_4)_2(H_2O)_6$].2H_2O	Brown	725.68	>300	85	23.15	4.69	3.85	15.39	13.3
	$C_{14}H_{34}N_2O_{20}Fe_2S_2$					(22.98)	(4.50)	(3.65)	(15.26)	
(17)	[(L)$(Cr)_2(SO_4)_2(H_2O)_6$].2H_2O	Brown	717.98	>300	85	23.39	4.74	3.89	14.48	15.5
	$C_{14}H_{34}Cr_2N_2O_{20}S_2$					(23.09)	(4.65)	(3.68)	(14.43)	
(18)	[(L)$(Cd)_2(OAc)_2$ $(H_2O)_6$].2H_2O	Brown	764.8	>300	82	28.24	5.23	3.66	29.39	15.6
	$C_{18}H_{40}Cd_2N_2O_{16}$					(28.15)	(5.01)	(3.54)	(29.05)	
(19)	[(H_2L)$(Cd)_2(SO_4)_2(H_2O)_6$].2H_2O	Brown	840.8	>300	73	19.98	4.28	3.33	26.74	15.2
	$C_{14}H_{36}Cd_2N_2O_{20}S_2$					(19.58)	(4.00)	(3.04)	(26.00)	
(20)	[(L)$(Cd)_2(Cl)_2(H_2O)_6$].2H_2O	Brown	717.7	>300	75	23.41	4.74	3.9	31.32	14.8
	$C_{14}H_{34}Cl_2N_2O_{12}Cd_2$					(23.02)	(4.06)	(3.2)	(31.00)	
(21)	[(L)CuZn$(OAc)_2(H_2O)_6$].2H_2O	Brown	669.44	>300	76	32.27	5.96	4.18	Cu=9.49 (9.0)	9.2
	$C_{18}H_{40}CuN_2O_{16}Zn$					(32.05)	(5.88)	(4.07)	Zn=9.84 (9.46)	
(22)	[(L)Zn$(OAc)_2Ni(H_2O)_6$].2H_2O	Drown	664.59	>300	66	32.5	6.01	4.21	Ni=8.83(8.32)	8.3
	$C_{18}H_{40}N_2NiO_{16}Zn$					(32.16)	(5.98)	(4.05)	Zn=9.92(9.62)	
(23)	[(L)MnZn$(OAc)_2(H_2O)_6$].2H_2O	Brown	660.83	>300	84	32.69	6.05	4.24	Zn=9.97(9.65)	14.8
	$C_{18}H_{40}MnN_2O_{16}Zn$					(32.6)	(5.89)	(4.07)	Mn=8.31(8.2)	
(24)	[(L)CoZn$(OAc)_2(H_2O)_6$].2H_2O	Brown	664.8	>300	88	32.49	6.02	4.21	Zn=9.91(9.35)	16.3
	$C_{18}H_{40}CoN_2O_{16}Zn$					(32.29)	(5.83)	(4.02)	Co=8.86(8.45)	

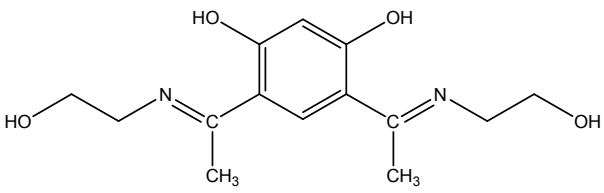

Ligand (1)

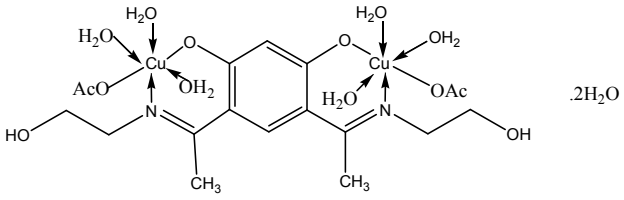

Complex (2)

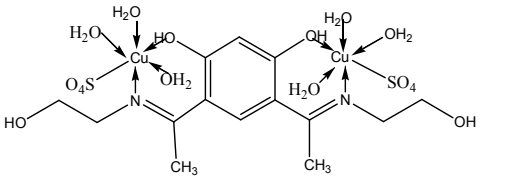

Complex (3)

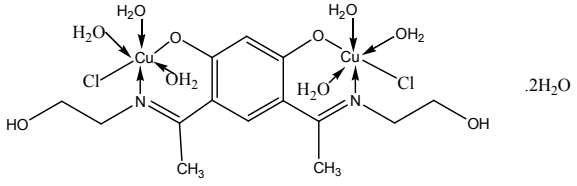

Complex (4)

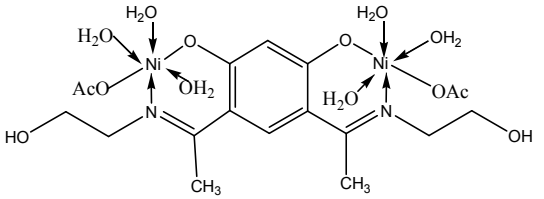

.2H2O

Complex (5)

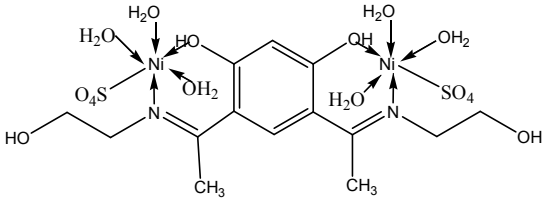

.2H2O

Complex (6)

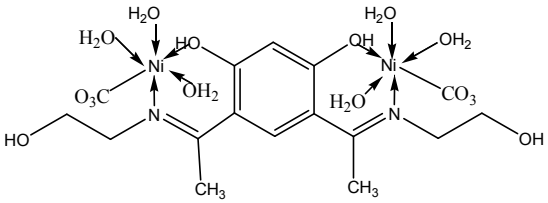

.2H2O

Complex (7)

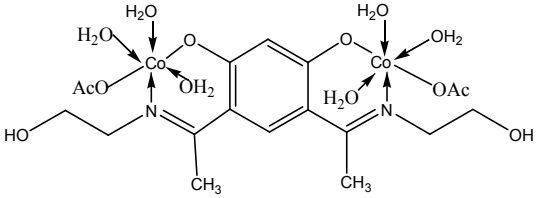

.2H2O

Complex (8)

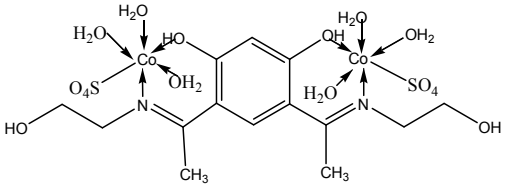

.2H2O

Complex (9)

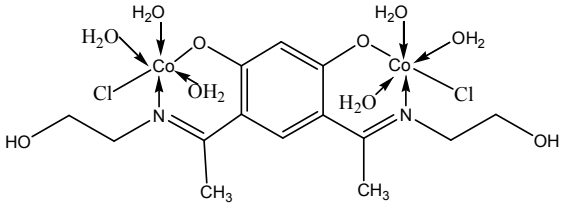

.2H2O

Complex (10)

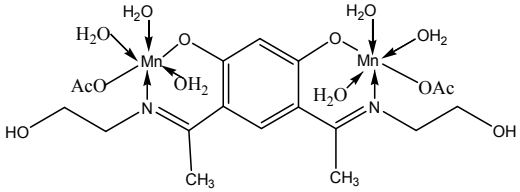

.2H2O

Complex (11)

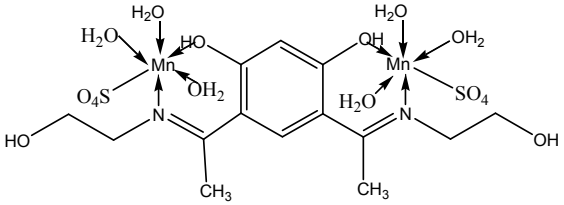

.2H2O

Complex (12)

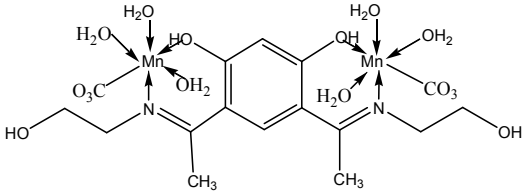

.2H2O

Complex (13)

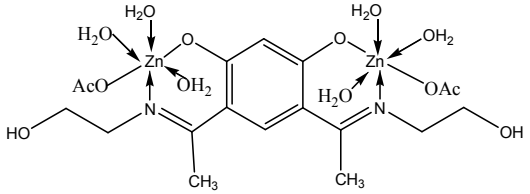

.2H2O

Complex (14)

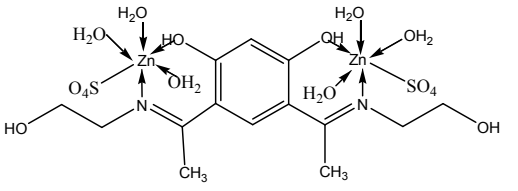

.2H2O

Complex (15)

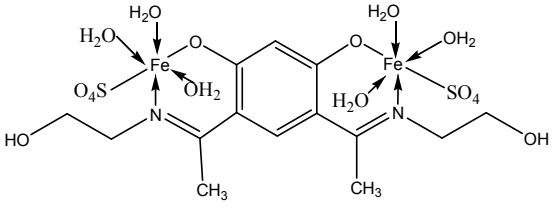

.2H2O

Complex (16)

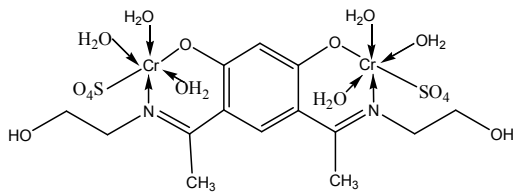

.2H2O

Complex (17)

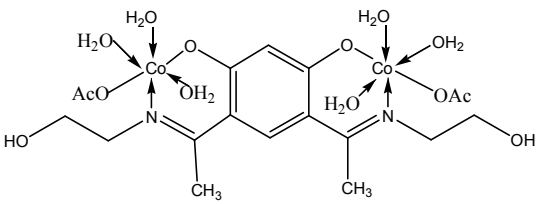

.2H2O

Complex (18)

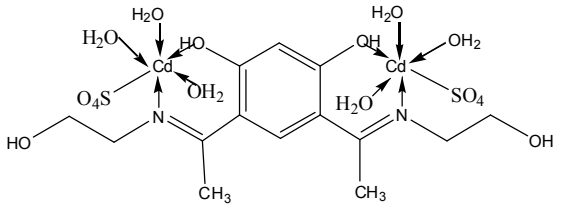

.2H2O

Complex (19)

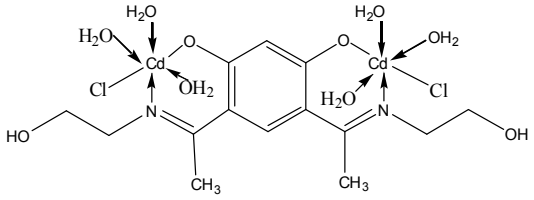

.2H2O

Complex (20)

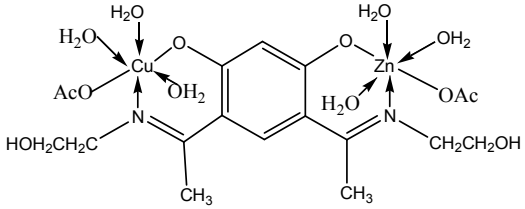

.2H2O

Complex (21)

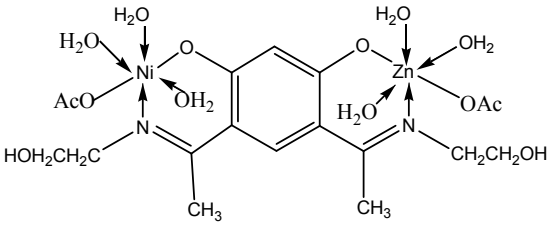

.2H2O

Complex (22)

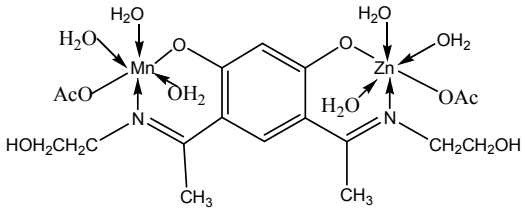

.2H2O

Complex (23)

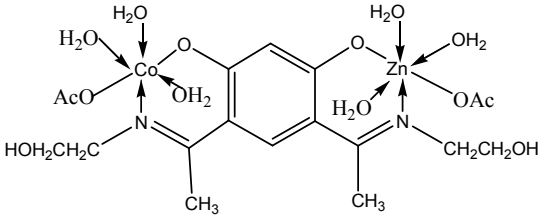

.2H2O

Complex (24)

Figure 1. Suggested chemical structures of ligand (1) and its metal complexes (2)-(24)

Standard	Ligand (1)	complex (3)	complex (4)	complex (10)	complex (11)	complex (12)	complex (16)	complex (17)
26.21	23.94	21.34	34.83	27.78	34.17	7.28	20.74	39.18

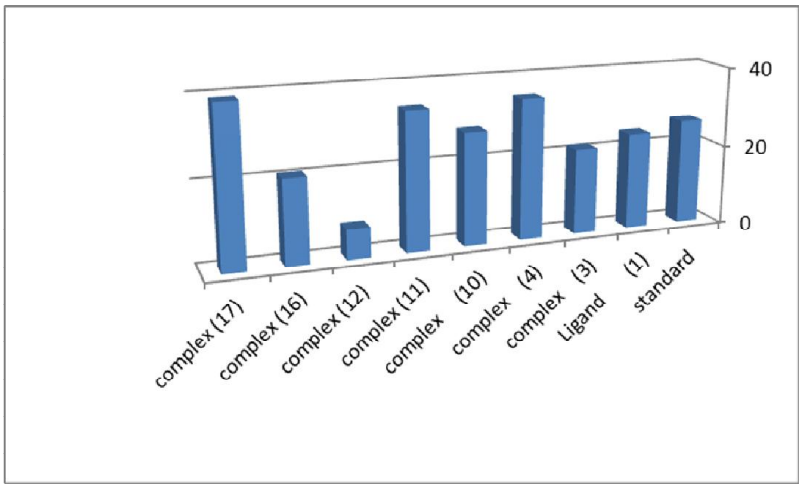

Figure 3. Antitumor effect of ligand (1) and complexes (3), (4), (10), (11), (12), (16) and (17) against HepG-2 liver cell line (50) µg/ml

Standard	Ligand (1)	complex (3)	complex (4)	complex (10)	complex (11)	complex (12)	complex (16)	complex (17)
18.89	34.82	37.02	41.64	40.97	43.68	18.93	38.95	52.72

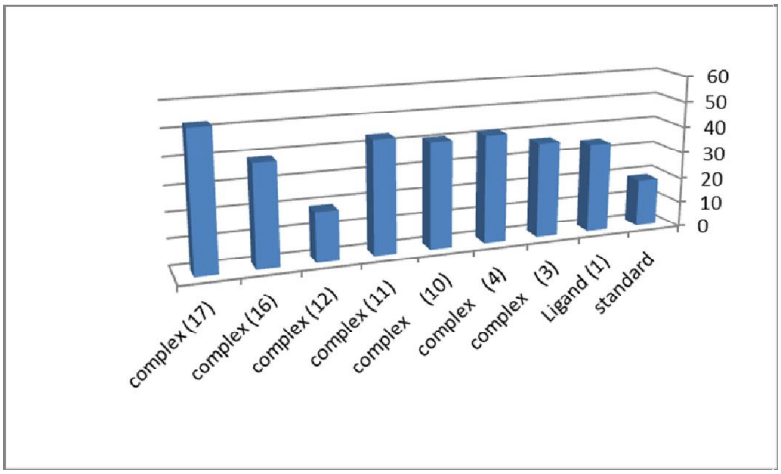

Figure 4. Antitumor effect of ligand (1) and complexes (3), (4), (10), (11), (12), (16) and (17) against HepG-2 liver cell line (25) µg/ml

Standard	Ligand (1)	complex (3)	complex (4)	complex (10)	complex (11)	complex (12)	complex (16)	complex (17)
21.19	56.76	53.18	70.69	61.83	52.94	26.51	71.87	68.49

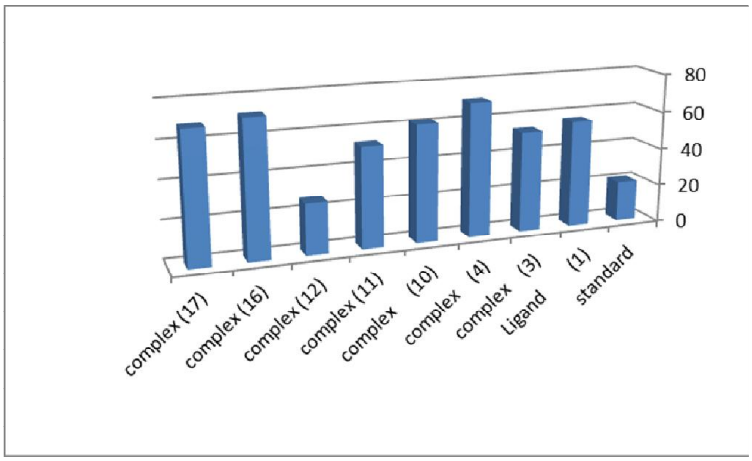

Figure 5. Antitumor effect of ligand (1) and complexes (3), (4), (10), (11), (12), (16) and (17) against HepG-2 liver cell line (12.5) µg/ml

Standard	Ligand (1)	complex (3)	complex (4)	complex (10)	complex (11)	complex (12)	complex (16)	complex (17)
31.18	70.62	69.49	86.18	75.28	71.82	39.44	78.53	82.5

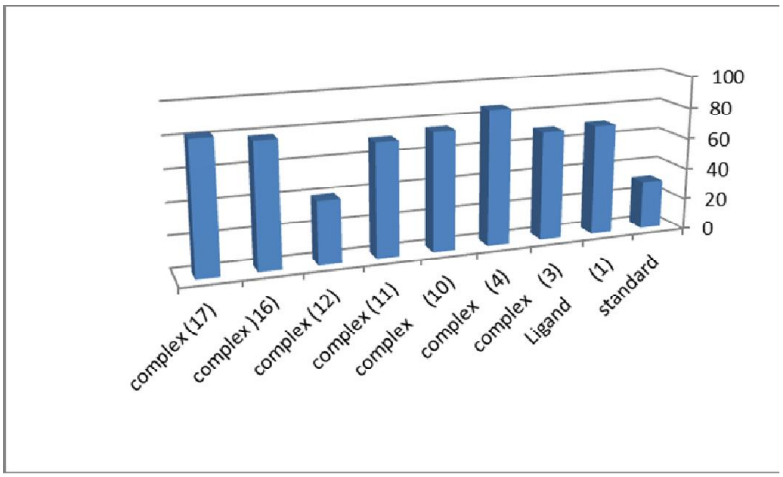

Figure 6. Antitumor effect of ligand (1) and complexes (3), (4), (10), (11), (12), (16) and (17) against HepG-2 liver cell line (6.25) µg/ml

Standard	Ligand (1)	complex (3)	complex (4)	complex (10)	complex (11)	complex (12)	complex (16)	complex (17)
73.12	87.19	84.27	92.73	89.17	86.55	52.87	94.16	91.67

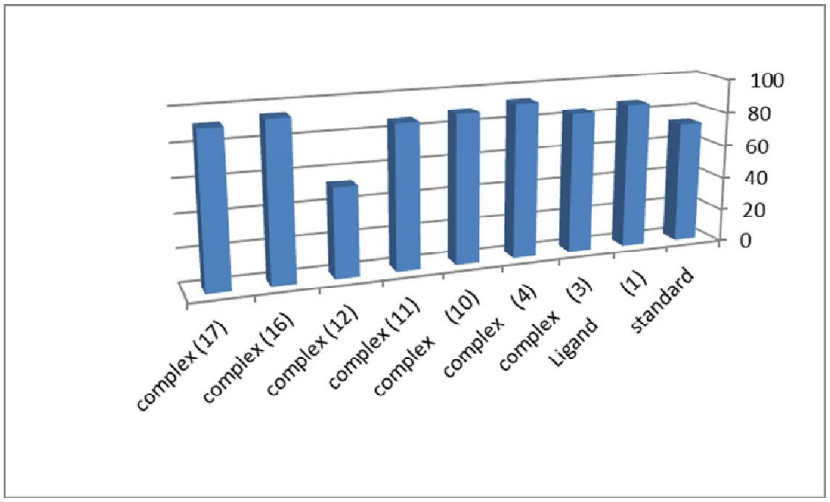

Figure 7. Antitumor effect of ligand (1) and complexes (3), (4), (10), (11), (12), (16) and (17) against HepG-2 liver cell line (3.125) µg/ml

Standard	Ligand (1)	complex (3)	complex (4)	complex (10)	complex (11)	complex (12)	complex (16)	complex (17)
88.5	96.56	96.5	97.92	94.29	92.89	78.19	98.72	95.43

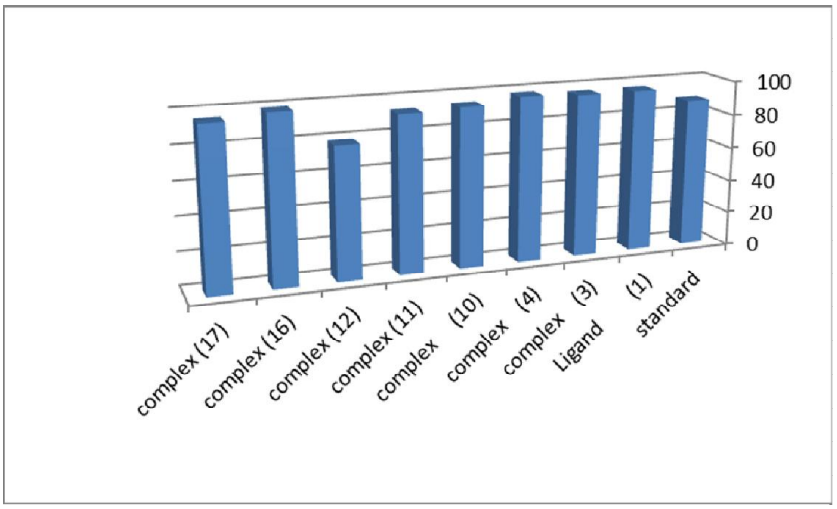

Figure 8. Antitumor effect of ligand (1) and complexes (3), (4), (10), (11), (12), (16) and (17) against HepG-2 liver cell line (1.56) µg/ml

	HepG-2
Ligand (1)	16.4
Complex (3)	15
Complex (4)	21.4
Complex (10)	19.6
Complex (11)	16.5
Complex (12)	3.79
Complex (16)	20.8
Complex (17)	30
Standard	3.73

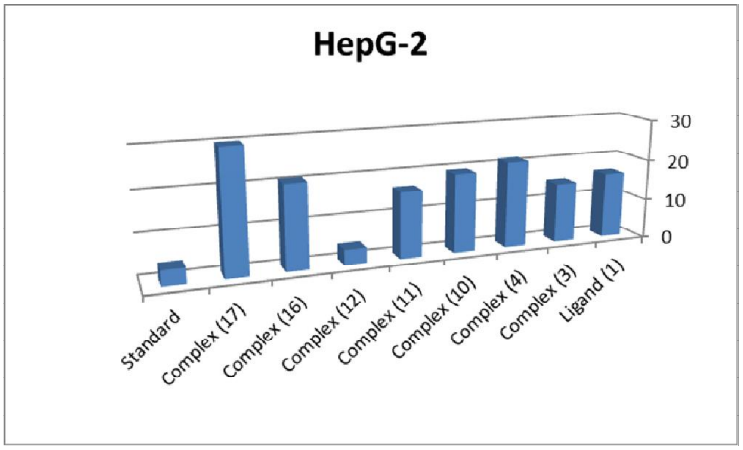

Figure 9. IC_{50} values of ligand (1) and complexes (3), (4), (10), (11), (12), (16) and (17) against human hepatocellular carcinoma cells (HepG-2)

Complex	S. pneumoniae	B. subtilis
Standard	23.8	32.4
Ligand (1)	16.6	14.3
Complex (3)	17.5	19.8
Complex (4)	17.2	14.9
Complex (10)	16.3	19.6
Complexv (11)	16.9	18.2
Complexv (12)	12.3	12.7
Complex (16)	12.9	13.2
Complex (17)	16.8	14.6
DMSO	0	0

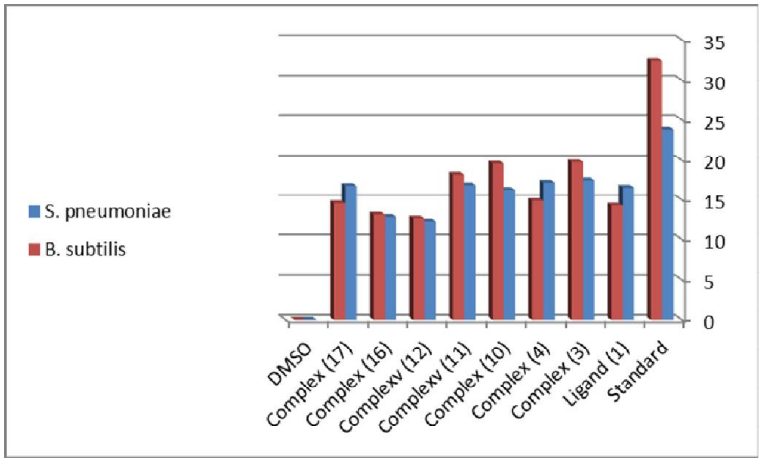

Figure 10. Antibacterial screening disc diffusion assay of ligand (1) and its metal complexes (3), (4), (10), (11), (12), (14), (16) and (17) using (5 mgl/ml) against S. pneumonia and B. subtilis

Complex	E. coli
Standard	19.9
Ligand (1)	9.4
Complex (3)	18.9
Complex (4)	16.2
Complex (10)	14.8
Complexv (11)	11.9
Complexv (12)	8.5
Complex (16)	10.8
Complex (17)	12.8
DMSO	0

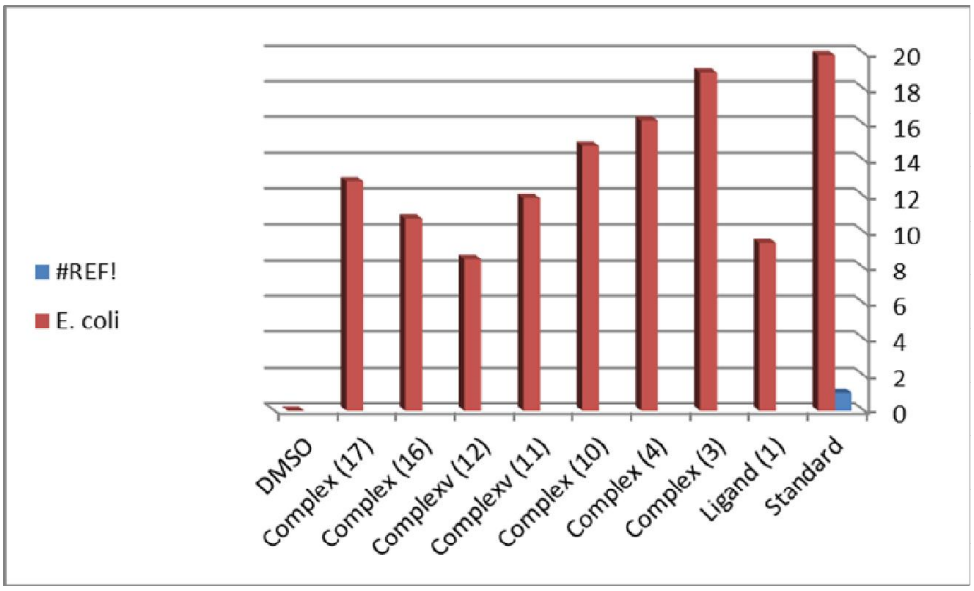

Figure 11. Antibacterial screening disc diffusion assay of ligand (1) and its metal complexes (3), (4), (10), (11), (12), (16) and (17) using (5 mgl/ml) against E. coli

Complex	A. fumigatus	C. albicans
Standard	23.7	25.4
Ligand (1)	13.6	11.7
Complex (3)	15.3	13.4
Complex (4)	16.25	14.1
Complex (10)	13.9	14.6
Complexv (11)	15.7	13.8
Complexv (12)	17.6	15.4
Complex (16)	18.7	16.9
Complex (17)	16.21	12.5
DMSO	0	0

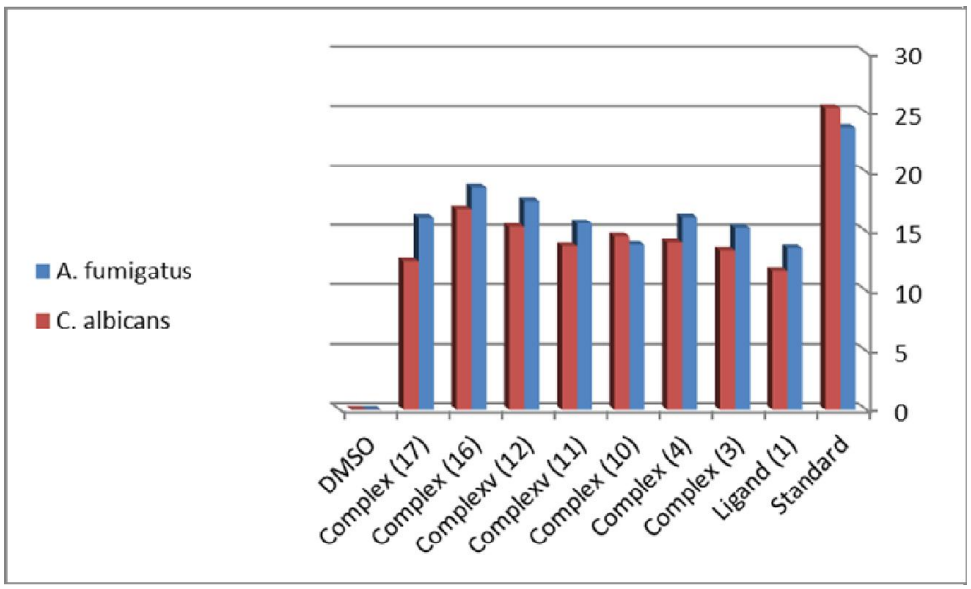

Figure 12. Antifungal screening disc diffusion assay of ligand (1) and its metal complexes (3), (4), (10), (11), (12), (16) and (17) using (5 mgl/ml) against A. fumigatus and C. albicans

Table 2. Mass spectra of the ligand (1) and its complexes (10), (16) and (21)

Ligand/ Compkex	m/z	Rel. Int.	Fragment
(1)	45	45	C_2H_5O
	86	41	C_4H_8NO
	177	91	$C_{10}H_{11}NO_2$
	194	17	$C_{10}H_{12}NO_3$
	235	41	$C_{12}H_{15}N_2O_3$
	280	45	$C_{14}H_{20}N_2O_4$
(10)	45	45	C_2H_5O
	86	41	C_4H_8ON
	250.35	163.35	$C_4H_{14}NO_5ClCo$
	340.35	90	$C_{10}H_{16}NO_6ClCo$
	488.7	148.35	$C_{10}H_{22}NO_9Co_2Cl_2$
	574.7	86	$C_{14}H_{30}N_2O_{10}Co_2Cl_2$
	610.7	36	$C_{14}H_{34}N_2O_{12}Co_2Cl_2$
(16)	45	45	C_2H_5O
	86	41	C_4H_8ON
	307.84	221.84	$C_4H_{14}NO_9Fe$
	381.84	74	$C_{10}H_{16}NO_9Fe$
	603.68	221.84	$C_{01}H_{22}NO_{17}Fe_2$
	689.68	86	$C_{14}H_{30}N_2O_{18}Fe_2$
	725.68	36	$C_{14}H_{34}N_2O_{20}Fe_2$
(21)	45	45	C_2H_{5O}
	86	41	C_4H_8NO
	278.54	129.54	$C_6H_{17}NO_7Cu$
	352.54	74	$C_{12}H_{19}NO_7Cu$
	547.44	194.9	$C_{14}H_{28}NO_{13}ZnCu$
	633.44	86	$C_{18}H_{36}N_2O_{14}ZnCu$
	669.44	36	$C_{18}H_{40}N_2O_{16}ZnCu$

Table 3. IR frequencies of the bands (cm^{-1}) of ligand [H_2L] and its metal complexes and their assignments

No.	ν(H_2O)	ν(OH)	υ(H-bonding)	ν(C=N)$_{imine}$	ν(Ar)	ν(OAc)/SO_4/CO_3)	υ(M-O)	υ(M-N)	υ(M-Cl)
(1)	-	3420, 3331	3640-3220	1652	1580, 870	-	-	-	-
			3130-2708						
(2)	3513-3240	3440, 3378	3657-3326	1624	1540, 860	1451, 1336	560	465	-
	3220-3040		3318-2955						
(3)	3630-3243	3450, 3415	3654-3275	1620	1534,766	1278,1150, 680	541	535	-
	3250-3170		3295-2780						
(4)	3526-3354	3430, 3420	3688-3150	1635	1560,764	-	570	532	450
	3175-3048		3127-2849						
(5)	3585-3356	3405, 3390	3620-3190	1626	1540, 835	1455,1355	543	479	-
	3168-3029		3157-2790						
(6)	3578-3353	3434, 3370	3694-3289	1608	1590, 834	1289, 1180, 670	535	440	-
	3184-3026		3368-2489						
(7)	3665-3354	3430, 3318	3680-3398	1623	1545, 790	1545,1364, 780	570	486	-
	3175-2806		3350-2870						
(8)	3590-3356	3465, 3315	3632-3477	1622	1525, 730	1448, 1366	525	470	-
	3165-3055		3210-2780						
(9)	3570-3288	3426, 3320	3680-3320	1626	1505, 735	1288, 1180, 680	580	508	-
	3285-2978		3329-2945						
(10)	3575-3325	3487, 3380	3660-3360	1638	1582,760	-	550	515	465
	3263-3125		3330-2770						
(11)	3550-3370	3470, 3306	3690-3324	1618	1590, 830	1475, 1349	563	505	-
	3270-3046		3320-2685						
(12)	3505-3205	3420, 3350	3659-3335	1625	1580, 763	1247, 1160, 690	580	480	-
	3345-3140		3318-2876						
(13)	3548-3277	3440, 3355	3658-3265	1626	1575, 830	1588,1340, 789	520	563	-
	3221-3065		3235-2789						
	3525-3367		3649-3398			1427, 1370		514	
(14)	3200-3078	3435, 3320	3340-2666	1610	1580, 815		589		-
(15)	3537-3314	3430	3630-3225	1609	1529, 769	1246, 1199, 670	545	526	-
	3265-3020		3208-2880						
(16)	3538-3339	3445, 3323	3640-3245	1613	1598, 750	1255, 1158, 680	578	515	-
	3226-3145		3229-2380						
(17)	3640-3283	3415, 3327	3620-3329	1620	1540, 870	1285, 1183, 658	534	490	-
	3385-2895		3350-2977						
(18)	3505-3318	3433	3660-3335	1624	1576, 790	1447, 1369	529	440	-
	3355-2880		3320-2950						
(19)	3670-3320	3422, 3330	3673-3289	1610	1573, 798	1255, 1135, 680	578	546	-
	3348-2980		3289-2820						
(20)	3510-3398	3430, 3366	3689-3277	1616	1555, 740	-	564	522	470
	3370-2840		3245-2389						
(21)	3560-3398	3440, 3338	3667-3188	1614	15540,789	1468, 1360	563	539	-
	3345-2770		3199-2674						
(22)	3550-3319	3450, 3320	3662-3108	1612	1530,788	1460, 1380	578	527	-
	3345-2984		3168-2699						
(23)	3580-3358	3488, 3316	3680-3134	1620	1560,750	1487, 1355	579	526	-
	3350-2870		3155-2799						
(24)	3579-3370	3477, 3370	3678-3168	1628	1568,760	1465, 1320	589	538	-
	3365-2975		3159-2609						

Table 4. The electronic absorption spectral bands (nm) and magnetic moment (B.M.) for the ligand [H_2L] and its complexes

No.	λ_{max} (nm)	μ_{eff} in B.M.
(1)	295 nm (log ε=4.05) , 400 nm (log ε =5.49)	-
(2)	270, 318, 390, 450, 530, 600	1.60
(3)	295, 302, 380, 460, 560, 650	1.67
(4)	280, 310, 350, 456, 510, 640	1.76
(5)	270, 313, 390, 505, 630, 725	3.39
(6)	275, 320, 380, 525, 635, 730	3.29
(7)	280, 310, 370, 515, 605, 720	3.26
(8)	270, 320, 375, 553, 628	4.72
(9)	278, 310, 376, 580, 620	4.71
(10)	275, 310, 360, 580, 650	4.83
(11)	270, 325, 370, 445, 565	5.11
(12)	270, 320, 378, 490, 558	5.08
(13)	277, 315, 410, 560	5.23
(14)	270, 280, 320, 395	Diam.
(15)	260, 290, 320, 380	Diam.
(16)	260, 335, 394, 465, 580, 660	5.18
(17)	285, 318, 389, 470, 560, 630	2.32
(18)	260, 330, 370	Diam.
(19)	280, 345, 380	Diam.
(20)	290, 315, 410	Diam.
(21)	275, 350, 470, 570, 640	1.72
(22)	260, 315, 375, 585, 620, 710	2.86
(23)	270, 325, 380, 460, 590, 610	5.16
(24)	285, 360, 390, 540, 620	4.22

Table 5. ESR data for the metal (II) complexes

No.	$g_{\parallel}$	$g_{\perp}$	g_{iso} [a]	$A_{\parallel}$ (G)	$A_{\perp}$ (G)	A_{iso} [b] (G)	G [c]	ΔE_{xy}	ΔE_{xz}	$K_{\perp}^2$	$K_{\parallel}^2$	K	$g_{\parallel}/A_{\parallel}$	α^2	β^2	β_1^2	-2 ß	a_d^2 (%)
(2)	2.13	2.04	2.07	130	10	50	3.25	18868	22222	0.51	0.36	0.68	163.8	0.54	0.94	0.67	147.5	62.8
(3)	2.18	2.05	2.09	150	15	60	3.6	17857	21739	0.63	0.48	0.76	155.7	0.63	1.0	0.76	178	75.7
(4)	2.20	2.05	2.1	145	10	55	4.0	19607	21929	0.63	0.58	0.78	157.1	0.65	0.97	0.89	149	63.5
(8)	-	-	2.09	-	-	-	-	-	-	-	-	-	-	-	-	-	-	-
(9)	-	-	2.1	-	-	-	-	-	-	-	-	-	-	-	-	-	-	-
(11)	-	-	2.007	-	-	-	-	-	-	-	-	-	-	-	-	-	-	-
(12)	-	-	2.009	-	-	-	-	-	-	-	-	-	-	-	-	-	-	-
(21)	2.16	2.04	2.08	150	15	60	4.0	17534	21276	0.48	0.42	0.68	154.3	0.60	0.8	0.7	165.4	70.36

a) $g_{iso} = (2g_{\perp} + g_{l})/3$, b) $Aiso = (2A_{\perp} + A_{l})/3$, c) $G= (g_{l} - 2)/ (g_{\perp} - 2)$

Table 6. Thermal data for the metal complexes

No.	Temp. (°C)	DTA (Peak)	TGA (wt. loss %)		Assignmenta
			Calc.	Found	
(2)	63	Endo	5.39	5.28	Loss of two hydrated water
	108	Endo	17.13	16.85	Loss of six coordinated water
	230	Endo	22.56	22.46	Loss of two acetate groups
	379	Endo	-	-	Melting point
	390, 424, 490, 617	Exo	39.27	39.02	Decomposition with formation 2CuO
(3)	60	Endo	4.84	4.53	Loss of two hydrated water
	127	Endo	15.57	15.41	Loss of six coordinated water
	250, 265	Endo	32.04	31.83	Loss of two coordinated sulphate groups
	373	Endo	-	-	Melting point
	480, 568, 619	Exo	39.07	38.81	Decomposition with formation of 2CuO
(10)	67	Endo	5.89	5.49	Loss of two hydrated water
	174	Endo	18.79	18.65	Loss of six coordinated water
	245	Endo	15.19	15.05	Loss of two chloride anions
	320	Endo	-	-	Melting point
	385, 444, 537, 635	Exo	37.85	37.56	Decomposition with formation of 2CoO
(14)	64	Endo	5.36	5.22	Loss of two hydrated water
	144	Endo	16.99	16.54	Loss of six coordinated water
	233	Endo	22.36	22.2	Loss of two coordinated acetate groups
	370	Endo	-	-	Melting point
	390, 407, 577, 684	Exo	39.97	39.78	Thermal decomposition with the formation of 2ZnO
(20)	60	Endo	5.01	4.81	Loss of two hydrated water
	123	Endo	15.84	15.64	Loss of six coordinated water
	217,	Endo	12.36	12.03	Loss of two chloride anions
	356	Endo	-	-	Melting point
	394, 465, 523, 744	Exo	51.07	50.78	Decomposition with formation of 2CdO

The antibacterial activity was tested against two bacterial strains: gram positive bacteria (*S.pneumonine* and *B.subtilis*) and gram negative bacteria (*E.coli*) strains. The results compared with standard drug (Tetracycline). The data indicated that, chelates were active against bacteria. Ligand and its metal complexes (3), (4), (10), (11), (12), (16) and (17) show antibacterial activities against gram positive bacteria (*S.pneumonine* and *B.subtilis*) and gram negative bacteria (*E.coli).* The results showed that, the metal complexes have a greater effect than ligand against bacteria (Ispir *et al.,* 2008). The relation between the inhibition mean zone of ligand (1) and metal complexes (3), (4), (10), (11), (12), (16) and (17) against *Stretococcs pneumoniae, Bacillis subtilis and Escherichia coli* are showed in Table (9), Figures (10 and 11).
Table (9A)

Antifungal activity

The ligand (1) and its metal complexes have been screened for their antifungal activities. The results show that, complexes (3), (4), (10), (11), (12), (16) and (17) have no effect on *Candida albicans and Aspergillus fumigmatus*. The order of the metal complexes is as shown in Table (10) and Figure (12). This enhancement in the activity can be explained on the basis of chelation theory. Chelation reduces the polarity of the metal ion considerably, mainly because of the partial sharing of its positive charge with donor groups and possible π-electron delocalization on the whole chelation ring. The lipid and polysaccharides are some important constituents of cell wall and membranes, which are preferred for metal ion interaction. In addition to this, the cell wall also contains many amino phosphates, carbonyl and cystenyl ligands, which maintain the integrity of the membrane by acting as diffusion and also provide suitable sites for bonding. Chelation can reduce not only the polarity of the metal ion, but also increases the lipophilic character of the complex and the interaction between metal ion and the lipid is favored. This may lead to the breakdown of the permeability barrier of the cell resulting in interference with the normal cell processes. Some important factors such as the nature of the metal ion, nature of the ligand, coordinating sites and geometry of the complex, concentration, hydrophilicity, lipophilicity and presence of co-ligands have considerable influence on antifungal activity. Certanly, steric and pharmacokinetic factors also play a decisive role in deciding the potency of an antifungal agent. Apart from this, the mode of the action of these compounds may also invoke hydrogen bond through the >C=N-N-CH- group with the active centers and thus interfere with normal cell process. The presence of lipophilic and polar substituents is expected to enhance antifungal activity. The antifungal activity of the ligand and its metal complexes were screened using the disk diffusion. The variation in the activity of different complexes against different microorganisms depends either on the impermeability of the cells of the microbes or differences in ribosomes in microbial cells.
Table (10):

MIC as alternative method in this work reported in µg/ml. Because of turbidity and or intense color of metal complexes solutions MIC was tested for antibacterial investigations. The minimum of MIC values against *Escherichia coli* was related to complex (4) (15.63 µg/ml) and complex (17) (62.5 µg/ml), but, MIC was tested for antifungal activity for complex (16) **(**500 µg/ml**)** against Aspergillus fumigatus.

Conclusion

Cr(III), Mn(II), Fe(III), Co(II), Ni(II), Cu(II), Zn(II) and Cd(II) complexes of Schiff base have been prepared and spectrally characterized. The IR data show that, the ligand behaves as dibasic tetradentate or neutral tetradentate**.** Molar conductances in DMF indicate that, the metal complexes are non-electrolytes. ESR spectra of solid Cu(II) complexes at room temperature show axial type (d_{x2-y2}) with covalent bond character in an octahedral environment. Complexes showed inhibitory activity against hepatocellular carcinoma (HepG-2 cell line). Also, the complexes show antibacterial activity and antifungal activities.

REFERENCES

Abu El-Reash, G. M., K. M. Ibrahim, M. M. Bekheit, Trans. 1990. *Met. Chem.* 15. 148

Ainscough, E. W., A. M. Brodie, A. J. Dobbs, J. D. Ranford, J. M. Waters, 1998. Inorg. Chem. Acta. 267. 27-38

Al-Hakimi, A. N., M. M. E. Shakdofa, A. M. A. El-Saidy, A. S. El-Tabl, 2011. *J. Kor. Chem. Soc.,* 55. 418

Baligar, R. S., V. K. Revankar, 2006. *J. Serb. Chem. Sac*., 71, 1301

Bauer-Siebenlist, A., F. Meyer, E. Farkas, D. Vidovic, S. Dechert, *J. Chem. Eur.*, 2005. 11. 4349-4360

Bhadbhade, M. M., 1993. D. Srinivas, *Inorg. Chem.* 32. 2458

Chang, H.Q., L. Jia, J. Xu, T.F. Zhu, Z.Q. Xu, R.H. Chen, T.L. Ma, Y. Wang and W.N. Wu. 2016. *J. Mol. Struct*., 1106, 366.

Chinvmia, G. C., D. G. Phillips, A. D. Rae, 1995. Inorg. *Chim. Acta.* 238,197-201

Chohan, Z. H., Sumrra, S. H., Youssoufi, M. H. & Hadda T B. Eur. J. Med. Chem., 45 (2010) 2739

Custot, J., J. L. Boucher, S. Vadon, C. Guedes, S. Dijols, M. elaforge,. Mansuy, 1995. *J. Biol. Inorg. Chem*. 1, 73

Dongli, C., J. Handong, Z. Hongyum, M. C. Degi, Y. Jina, L. B. Jian, 1994. Polyhedron, 13, 57.

Duda, B. M., A. Karaczyn, H. Kozlowski, I. O. Fritsky, T. Glowiak, E. V. Prisyazhnaya, T. Y. Sliva, J. S. Kozlowskac, 1997. *J. Chem. Soc. Dalton Trans,* 3853.

Durai Anad, T., Pothiraj, C., Gopinath, R. M. and Kayalvizhi, 2008. *B. Afr. J. Microb. Res.,* 2. 63

El- Tabl, A. S. & Shakdofa, M. M. E. 2013. *J. Serb. Chem. Soc.,* 78, 39

El-Bahnasawy, R. M., A. S. El-Tabl, E. El-Sheroafy, T. I. Kashar, Y. M. 1995. Issa, *Polish J. Chem.* 73.

El-Behry, M., M. El-Twigry, 2007. *Spectrochim Acta*. Part A 66, 28.

El-Boraey, H. A., A. S. El-Tabl, 2003. *Polish J. Chem*. 77 1759-1775

El-Tabl, A. S., 1997. Transition Met. Chem. 22. 400-500

El-Tabl, A. S., 2004. *Bull. Korean Chem. Soc*. 25 1-6

El-Tabl, A. S., F. A. El-Said, A. N. Al-Hakim, W. 2007. *Plass, Trans. Met. Chem.* 67, 265

El-Tabl, A. S., F. A. El-Said, A. N. Al-Hakim, W. Plass, 2007. *Trans. Met. Chem.*, 67, 265.

El-Tabl, A. S. 2004. *J. Chem. Reas.,* 19

El-Tabl, A. S. 2002. *J. chem. Reas.*, 22, 595-532

El-Tabl, A. S. 2002. *J. Chem. Res.*, 529.

El-Tabl, A. S., K. El-Baradie, R. M. Issa, 2003. *J. Coord. Chem.*, 56, 1113.
El-Tabl, A. S., M. M. Abou-Sekkina, 1999. *polish J. Chem.*, 73,1937-1945
El-Tabl, A. S., M. M. E. Shakdofa, A. M. A. El-Seidy, 2011. *Korean J. Chem. Soc*., 55, 603
El-Tabl, A. S., S. A. El-Enein, 2004. *J. Coord. Chem.*, 57, 281
El-Tabl, A. S., S. M. Imam, 1997. *Trans. Met. Chem.* 22, 259
El-Tabl, A. S. 2002. *Trans. Met. Chem.*, 27, 166.
El-Tabl, A. S. 1998. *Trans. Met. Chem.,* 23, 63
El-Tabl, A. S., 1997. *Transition Met. Chem.,* 22, 400.
El-Tabl, A.S., F. A. El-Saied, A. N. Al-Hakimi, 2008. *J. Coord. Chem.* 61, 2380-2401
El-Tabl, S., R. M. El-Bahnasawy, M. M. E. Shakdofa, E. El-Deen Abdalah, 2010. *J. Chem. Reas.,* 88.
Feng, G., J. C. Mareque-Rivas, R. T. Rosales, N. H. Williams, 2005. *J. Am. Chem. Soc.*,127,13470-13471
Fouda, M. F. R., M. M. Abd-El-Zaher, M. M. Shakdofa, F. A. El-Sayed, M. I. Ayad, A. S. El-Tabl, 1983. *J. Coord. Chem.* 61, 1983.
Gaber, M., M. M. Ayad, 1991. *Thermochim Acta.* 176, 21-29
Gaetke, L. M., C. K. Chow, 2003. Toxicology 189, 147-163
Geary, W. 1971. *J. Coord. Chem. Rev.* 7 81-122
Gudasi, K. B., M. S. Patil, R. S. Vadavi, R. V. Shenoy, S. A. Patil, M. Nethayi, 2006. *Trans. Met. Chem.* 31. 580-585
Gudasi, K. B., S. A. Patil, R. S. Rashmi, V. Shenoy, M. Nethaji, 2006. *Trans. Met. Chem.,* 31. 580
Gudasi, K. B., S. A. Patel, R. S. Vadvavi, R. V. Shenoy, M. Nethayi, *Trans. Met. Chem.,* 31, 586.
Hall, I. H., C. C. Lee, G. Ibrahim, M. A. Khan, G. M. Bouet, 1997. *Appl. Organomet. Chem.*, 11, 565-575
Hegazy, W. H. 2001. *Monatsch Chem*., 132, 639.
Illan – Cabeza, N. A., A. R. Garcia – Garcia, M. N. Moreno – carretero, J. M. Martinez – Martos, M. I. Ramirez – exposito, 2005. *J. Inorg. Biochem.,* 99, 1637-1645
Ispir, E., S. Toroglu, Z. A. Kayraldi, 2008. Transition Met Chem. 33, 953
Kantekin, H., U. Ocak, Y. Gok, H. 2004. *Alp, J. Coord. Chem*. 57, 265
Kivelson, D., R. Neiman, 1961. *J. Chem. Phys.* 35, 149-155
Klement, R., F. Stock, H. Elias, H. Paulus, P. Pelikan, M. Valko and M. Mazur, 1999. Polyhedron, 18, 3617.
Krishna, A. H., C. M. Mahapatra, K. C. Dush, 1997. *J. Inorg. Nucl. Chem.*, 39,1253
Kumar, M.P., S. Tejaswi, A. Rambabu, V.K.A. Kalalbandi and Shivaraj Polyhedron, 2015. 102, 111.
Kuska, H. A., M. T. Rogers, 1971. Coordination Chemistry Martell AE Ed: Van Nostrad Reihoid Co New York, 92.
Lever, A. B. P. 1986. Inorganic Electronic Spectroscopy Elsevier pub Company New York, 275-283
Lewis, J., R. G. Wilkins, Modern. 1960. Coordination. Chemistry. Interscience. New. York. 40, 403-406
Mahapatra, B. B., B. K. Mahapatra, 1997. *J. Inorg. Nucl. Chem.*, 39, 2291.
Mareque, J.C., R. Prabaharan, S. Parsons, 2004. Dalton Trans. 21,1648-1655
Motaleb, A. E., M. Ramadan, W. Sawodny, H. Baradie, M. Gaber, 1997. *Trans. Met. Chem.*, 22, 211-215
Nagesh, G.Y., K. Mahendra Raj and B.H.M. Mruthyunjayaswamy, 2015. *J. Mol. Struct.,* 1079, 423.
Naiya, S., H.S. Wang, M.G.B. Drew, Y. Song and A. Ghosh, 2011. Dalton Trans., 40, 2744.
Nakatamato, K.,1967. Infrared spectra of Inorganic and Coordination compounds 2nd End Wiley Inc New York.
Nickless, D. E., M. J. Power, F. L. Urbach, 1983. *Inorganic Chem.* 22, 3210-3217
Omar, M.M., G.G. Mohamed and A.A. Ibrahim, 2009. *Spectrochim. Acta A*,73, 358.
Parihari, R. K., R. K. Patel, R. N. Patel, 2000. *J. Ind. Chem. Soc.*, 77, 339
Plass, W., A. S. El-Tabl, A. Pohlman, Coord. 2009. *Chem.,* 62 358-372
Procter, I. M., B. J. Hathaway, P. N. Nicholls, 1969. *J. Chem. Soc. A*, 1678-1684
Rahaman, F. and B.H.M. Mruthyunjayaswamy, Complex Metals, 1, 88 (2014).
Raman, N. and S. Sobha, 2012. *Inorg. Chem. Commun.,* 17, 120.
Ray, R. K. 1990. *Inorg. Chim. Acta*. 174, 257
Rouzer, A. A., 2010. Chemical. Research in Toxicology 23, 1517-1518
Sakamoto, S. Itose, T. Ishimori, N. Matsumoto, H. Okawa and S. Kida, 1990. *Bull. Chem. Soc. Jpn.,* 63, 1830.
Sallam, S. A., A. S. Orabi, B. A. El-Shetary, A. Lentz, 2002. *Trans. Met. Chem.* 27, 447
Sedighinia, F., Safipour Agshar A., Soleimanpour Zarif, S. R., Asili, J., Ghazvini, K. & Avicenna, 2012. *J. Phytomed.,* 2 (2012) 118
Singh, N. K., S. B. Singh, Transition Met. Chem. 26 (2001) 487-495
Skehan, P., R. Storeng, *et al*, 1990. *J. Natl, Cancer Inst*. 82,1107
Smith, D. W. 1971. *J. Chem. Soc. A*., 3108-3120
Symons, M.C.R. 1979. Chemical and Biological Aspects of Electron Spin Resonance Van Nostrand Reinhold Wokingham.
Takkar, N. V., S. Z. Bootwala, *Indian J. Chem.* 1995. 34A, 370-374
Tas, E., A. Cukuroval, 1999. *J. Coord. Chem.*, 1999, 47, 425.
Tas, E., M. Aslanoglu, A. Kilic, Z. Kara, 2005. *Trans. Met. Chem.*, 30, 758 .
Vogel, I., 1961. A text Book of Quantitative Inorganic Analysis (Longman Suffolk).
Zafar, H., A. Ahmad, A.U. Khan and T.A. Khan, 2015. *J. Mol. Struct.,* 1097, 129.
Zayed, E.M., G.G. Mohamed and A.M.M. Hindy, 2015. *J. Therm. Anal. Calorim.,* 120, 893 (2015).

****